ORIGINAL ARTICLE

COMPARATIVE CORROSION INHIBITION STUDY OF ORDINARY STEEL IN 1M HCl DL- α -ALANINE AND BIS $Ni(ALA)_2Cl_2$ COMPLEX SYNTHESIS

| Nadia Gharda [1*] | Mouhsine Galai [2] | Lamyae Saqalli [1] | Moussa Ouakki [3] | Rachida Ghailane [1] | Mohamed EbnTouhami [2] | Abdelaziz Souizi [1] | and | Nouzha Habbadi [1] |

[1.] Laboratory of Organic, Organometallic and Theoretical Chemistry | Faculty of Science | University Ibn Tofail | BP. 133-14000, Kenitra | Morocco |
[2.] Laboratory of Materials Engineering and Environment: Modeling and Application, Faculty of Science | University Ibn Tofail BP. 133-14000, Kenitra | | Morocco |
[3.] Laboratory of materials, electrochemistry and environment | Faculty of Science, Ibn Tofail University | PB 133-14050 Kénitra | Morocco |

| Received | 12 March 2019 | | Accepted 12 April 2019 | | Published 19 April 2019 | | ID Article | Nadia-ManuscriptRef.6-ajira2970319 |

ABSTRACT

Background: Metallic ions such as nickel are essential elements present in many species (proteins..). However, an excess of these ions in the human body can seriously affect our health. Furthermore, Nickel (II) is capable of reacting with mono-, bi- and polydentate ligands to form complex compounds with various applications (environmental, biological and medical). **The aims:** we present in this paper the synthesis and the characterization of nickel (II) complex using alanine as ligand, after that the ligand and the obtained complex were tested in the environment field as anticorrosive agents. **Material and methods:** the complexation of alanine with anhydrous nickel chloride was studied. The isolated complex $Ni(ala)_2Cl_2$ with a yield equal to 82% was characterized by the UV-visible spectroscopy, the infrared spectroscopy and the scanning electron microscopy (SEM) energy dispersive X-ray (EDX) analysis. The synthesized complex $Ni(ala)_2Cl_2$ and the ligand alanine on the corrosion of ordinary steel in 1M HCl solution was then evaluated by means of stationary and transient electrochemical methods (stationary and transient). A comparative study of their anticorrosive activities was also performed. **Conclusion:** The complex $Ni(ala)_2Cl_2$ synthesis was found to be possessing highest inhibitory effect with 95% at 10-3M. The results obtained showed that the dissolution rate of the metal depends on the molecular structure and the concentration of product.
Keywords: *DL-α-alanine, complexation, Ni(ala)2Cl2, corrosion, inhibitor* .

1. INTRODUCTION

Amino acids are the chemical units of proteins, which construct the structure for all living organism 1 and essential for various biochemical processes that support the maintaining of life in the individuals 2. They are good chelating agents 3 and can coordinate to transition metals through their amino or carboxylic groups [1, 2, 3 ,4]. During the last few decades the complexation of transition metal ions with amino acids have been studied [5, 6, 7, 8]. The amino acid-metallic ion interactions are found to be responsible for enzymatic activity and stability of protein structures [9, 10, 11].

The formed complexes have also corrosion inhibition effects, but little works are done for this application [12, 13, 14, 15]. Indeed, the corrosion phenomenon concerns most industrial sectors including the aeronautics industry, automotive and the chemical and petrochemical industries [16]. The economic stakes are considerable. Corrosion is not only a waste of raw materials and energy but can also cause serious accidents and often contribute to environmental pollution [17]. The acids are the most used agents in many industrial processes, causing metal degradation and metal aggression by chemical or electrochemical reactions [18, 19].

Our objective is to synthesize the Ni(ala)2Cl2 complex from ligand alanine with good yield. This complex and ligand have the advantages of being soluble in aqueous media and no toxic. After purification, the complex is analyzed by Nuclear Magnetic Resonance (RMN), the UV-visible spectroscopy, the infrared spectroscopy and the scanning electron microscopy (SEM) energy dispersive X-ray (EDX) analysis. We are interested in studying the behaviour of steel in HCl 1M, and to determine the inhibitory efficacy of two compounds alanine and complex who presented inhibitory effects of ordinary steel corrosion in 1M HCl. Electrochemical measurements were carried out to conduct this study.

***Corresponding author & Author Copyright © 2019:** | **Nadia Gharda** |

2. Experimental

2.1. Instruments

Infrared spectra (KBr disks) were recorded IRTF Vertex 70 Infrared Spectrophotometer in the range of 4000 to 400 cm^{-1}.

The UV-visible spectrophotometric studies were performed in the range of 200-800 nm by using an SP-2000UV Spectrophotometer with a 1 cm cell at a concentration of 10^{-3}M in water at room temperature.

The recording of Nuclear Magnetic Resonance spectra was performed on a Bruker Advanced 300 WB at 300 MHz for solutions in D2O and chemical shifts are specified in δppm with reference to tetramethylsilane (TMS) as an internal standard.

The observation using a scanning electron microscope (VEGA3 TESCAN) coupled with EDX analyzes. These analyzes were done at the Semlalia University of Marrakesh.

2.2. The preparation of the Ni(II) complex with the amino acid (DL-α-alanine)

The Ni(ala)2Cl2 was synthesized according to the classical literature method 20. This complex is prepared with stirring at room temperature. 2 mmoles of alanine dissolved in 20 ml of water was introduced into an erlenmeyer flask. 2 mmoles of triethylamine was added to deprotonate the amino acid. A solution consisting of 1 mmoles of nickel chloride hexahydrate in 10 ml of water was added drop wise with the aid of a burette. When the addition was complete, the reaction is kept under stirring at room temperature for 8 hours.

A precipitate formed. The blue precipitate was filtered on a frit with a vacuum flask and washed with ethanol. A light blue powder was obtained and was dried in an oven at 60°C. The calculated yield from the obtained dry powder is equal to 82%.
The obtained solid was recrystallized from a mixture (1/2) H_2O / EtOH, light blue crystals appear.

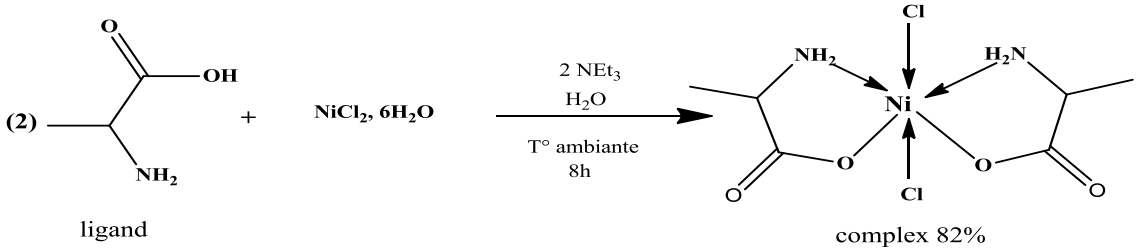

ligand — complex 82%

Scheme: reaction of the complexation of alanine with nickel.

2.3. The used materials

The chemical composition of ordinary steel tested in this study is given in Table 1.

Table 1: Mass Chemical Composition of Ordinary Steel

Elements	**C**	**Si**	**Mn**	**Cr**	**Mo**	**Ni**	**Al**	**Cu**	**Co**	**V**	**W**	**Fe**
Teneur (%)	0.11	0.24	0.47	0.12	0.02	0.1	0.03	0.14	<0.0012	<0.003	0.06	98.7

2.3.1. Inhibitors

Ligand (alanine)
Complex ($Ni(ala)_2Cl_2$)

2.3.2. Solution

The aggressive solution of 1M HCl prepared by dilution of the commercial solution hydrochloric acid (37 %) with distilled water.

2.4. Electrochemical measurements

The electrochemical experiments are carried out in a pyrex cell equipped with a conventional three-electrode assembly: steel ($1cm^2$) as working electrode (ET), platinum as auxiliary electrode and Ag/AgCl electrodes as reference electrodes.

The intensity-potential curves are obtained in the potentiodynamic mode. The potential applied to the sample varies continuously with a scanning rate of 1MV/s.

We have chosen a relatively low scanning speed so as to be in the quasi-stationary mode. The measurements are made with a mounting including a galvanostat potentiometer PGZ100, of radiometer type, associated with the Voltamaster 4 software. Before the curves are plotted, the working electrode is maintained for 30 minutes at its abort potential. We first plotted the cathodic curves and then the anodic curves.

3. RESULTS AND DISCUSSIONS

3.1. Analyzing methods of the complex $Ni(ala)_2Cl_2$

The synthesized complex is solid that is present in the form of a colored powder. It is very stable to air and room temperature. Their melting point is high and more than 260 ° C.

The structure of the complex was determined from the following spectral data: IR spectroscopy, UV-visible spectroscopy, Nuclear Magnetic Resonance (RMN) and scanning electron microscopy (SEM) energy dispersive X-ray (EDX) analysis.

3.2. Infrared Spectroscopy

Table 2, brings together the main infrared bands observed for the synthesized complex and ligand.

Table 2: the main infrared absorption bands of ligand (alanine) and complex (Ni(ala)2Cl2).

bands	ligand	complex
v (N-H)	3037	3094
vas (C=O)	1593	1559
vs (C=O)	1410	1330
v (Ni-O)	---	462
v (Ni-N)	---	573

The comparative study of the infrared spectra of the ligand and those of the complex makes it possible to notice that:

- In the spectrum of the complex $[Ni(ala)_2Cl_2]$ (Fig.1.a) the displacement of the characteristic bands $v(NH_2)$ towards the higher energies 3094 cm-1 suggest the coordination of the amino acids with the nitrogen of the amine group. In alanine (Fig.1.b), two absorptions related to the two asymmetric and symmetric vibration modes are characteristic of the carboxyl ion COO-[20]. In the alanine complex, the asymmetric v(C=O) vibration band moves from 1593 à 1559 cm-1 and the symmetrical vibrating band v(C=O) moves from 1410 à 1330 cm-1. The slipping of the position of the bands v(C=O)as and v(C=O)s in the complex with respect to the ligand suggests that alanine is coordinated with nickel by the COO- group [21,22].
- We also see the appearance of new bands in regions 460-496 cm-1 and 525-590 cm-1, due respectively to v(M-N) and v(M-O)[23,24,25,26].

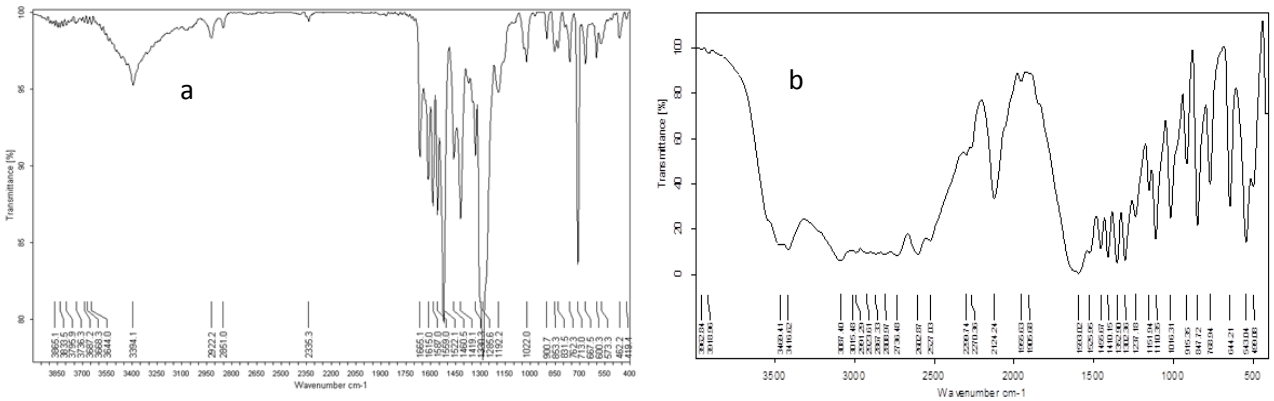

Figure 1: Spectrum IR of the complex $Ni(ala)_2Cl_2$(a) and ligand the ligand alanine (b) in KBr.

3.3. The UV-visible spectrophotometry

The electron spectrum of nickel (II) complex and ligand alanine was recorded in water at the concentration of 10^{-3} M. The obtained results are summarized in Table 3.

Table 3: The table presents thehe main bands of the ligand and the complex electron spectrum.

	λ max (nm)	ν (cm-1)	εmax (l.mol^{-1}.cm^{-1})	Transition
Ligand	322	31060	7	n → π *
	389	25710	31	n → π *
Complex	893	11199	163	d - d
	629	15899	164	d - d
	389	25710	335	L → M

Where **ν** : wave-number cm^{-1}, **λ** : Wavelength (nm), **ε** : molar absorption coefficient (mol^{-1}. L .cm^{-1})

The UV-Visible electron spectrum of the ligand (Fig.2.a) in water has two bands: one at 322 nm and the other at 389 nm. These bands are attributed to the transition n →π* [27].

The value of the complex (Fig.2.b) molar absorption coefficient (ε) indicates that it has an octahedral geometry. This value is compatible with those reported in the bibliography [28,29,30]. The transitions bands $^3A_{2g} \rightarrow {}^3T_{1g}$ (F) and $^3A_{2g} \rightarrow {}^3T_{2g}$ (F) [31,32,33] appear at 629 and 893 nm.

These are d-d transitions. The band 389 nm is attributed to the ligand-metal charge transfer (L→M) of a d^8 configuration [34,35,36].

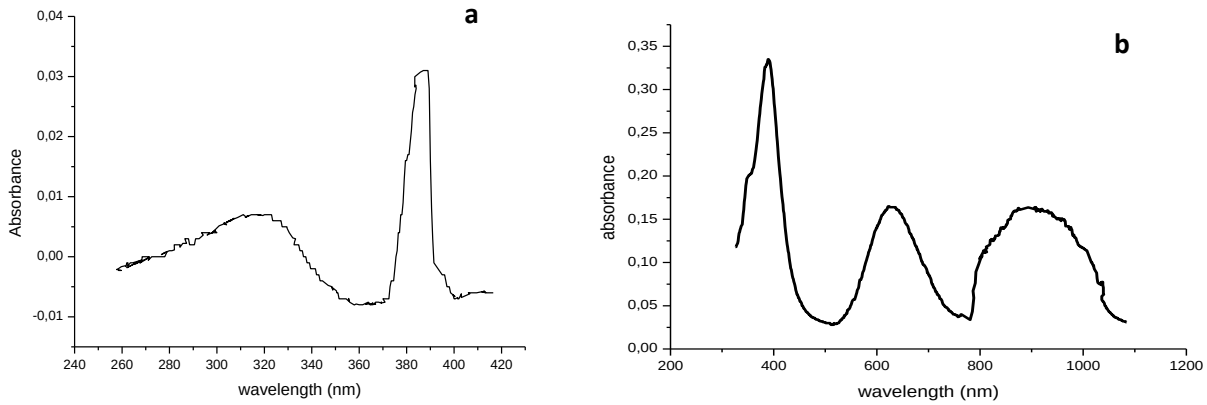

Figure 2: UV-Visible Spectra of alanine (a) and $Ni(ala)_2Cl_2$ complex (b).

3.4. Nuclear Magnetic Resonance (RMN)

The structure of the Nickel complex was identified using ^{1}H NMR and ^{13}C NMR spectroscopy

- **^{1}H NMR spectrum :**

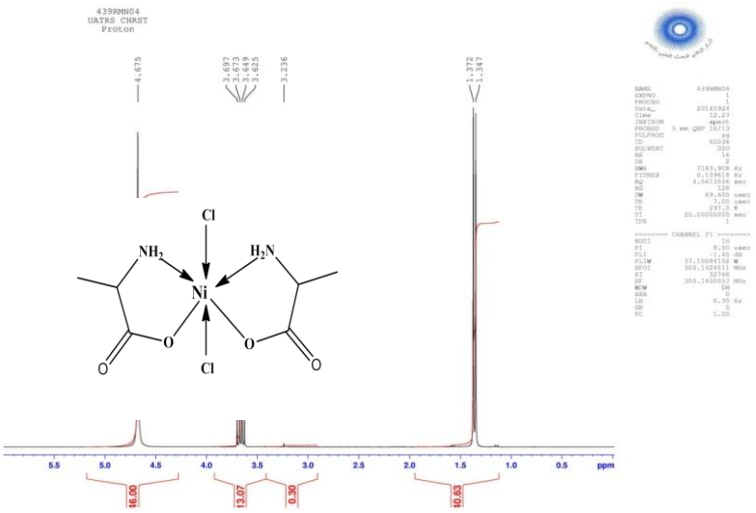

Figure 3: 1H NMR spectra of Nickel complex.

The 1H NMR spectra of Nickel complex in D_2O (Fig.3), showed the following signals

- A doublet at 1.35 ppm attributable to the proton of the methyl group.

- A quadruplet at 3.65 ppm attributable to the proton of the CH group.
- A singlet at 4.67 ppm attributable to the two proton of the NH_2 group.

The 1H-NMR spectrum shows the absence of Hydrogen of the carboxylic acid function. The disappearance of Hydrogen can be explained by the formation of complexation by reaction between alanine and nickel.

- **^{13}C NMR spectrum :**

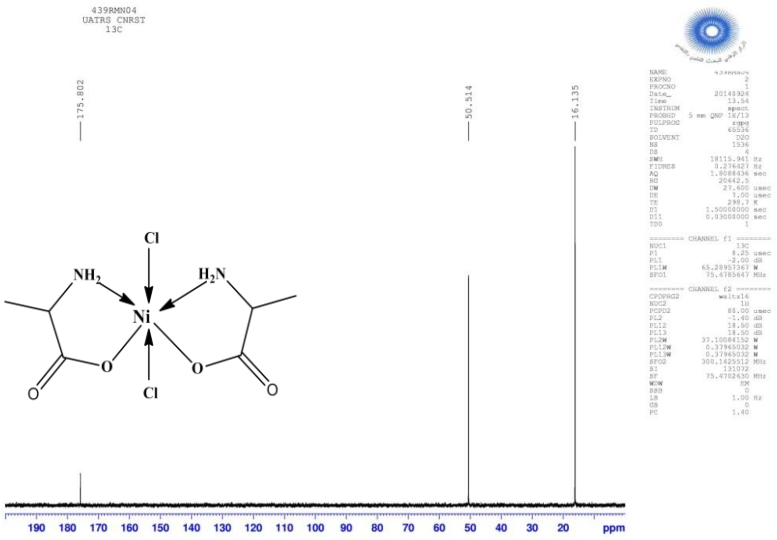

Figure 4: ^{13}C NMR spectra of Nickel complex.

The ^{13}C NMR spectrum (Fig.4) shows in the Sp^3 carbon region a first signal at 16.1 ppm is attributed to the carbon of the methyl group. A second signal at 50.5 ppm is attributed to the CH group. Also in the carbon region Sp^2 there is a signal at 175.8 ppm corresponds to the C=O group.

- **DEPT Spectrum:**

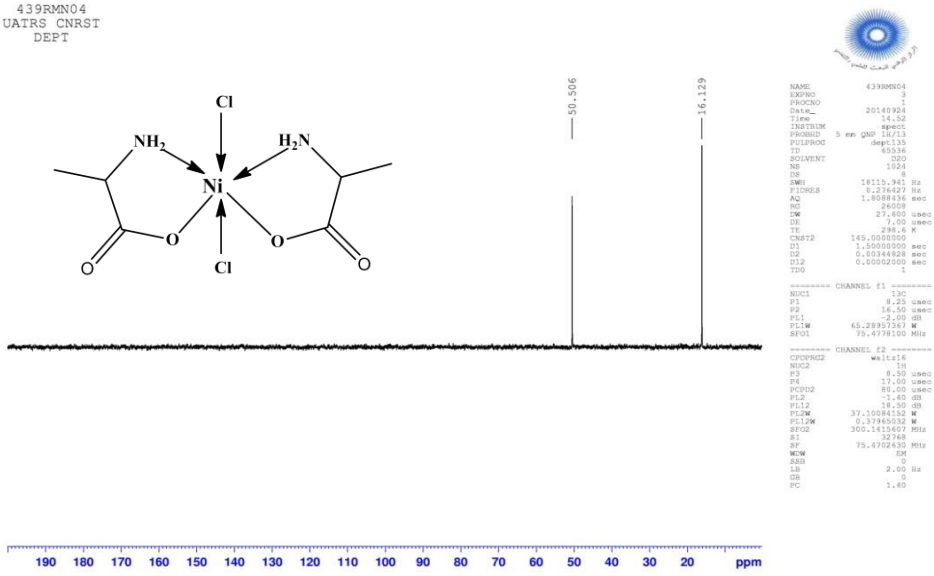

Figure 5 : DEPT spectra of Nickel complex.

The analysis of the DEPT spectrum (Fig.5) confirms the results obtained previously in the ^{13}C NMR spectrum, It shows that the signals (16.1 ppm and 50.5 ppm) are not affected, which confirms that it is secondary carbon. On the other hand, the absence of the signal at 175.8 ppm proves that it is a quaternary carbon.

3.5. Scanning electron microscopy (SEM) energy dispersive X-ray (EDX) analysis

The analysis by MEB and EDX is carried out using a VEGA3 TESCAN branded device. This monocrystal analysis of the phase obtained confirms the presence of elements Ni, Cl, O and N in the structure (Scheme 1).

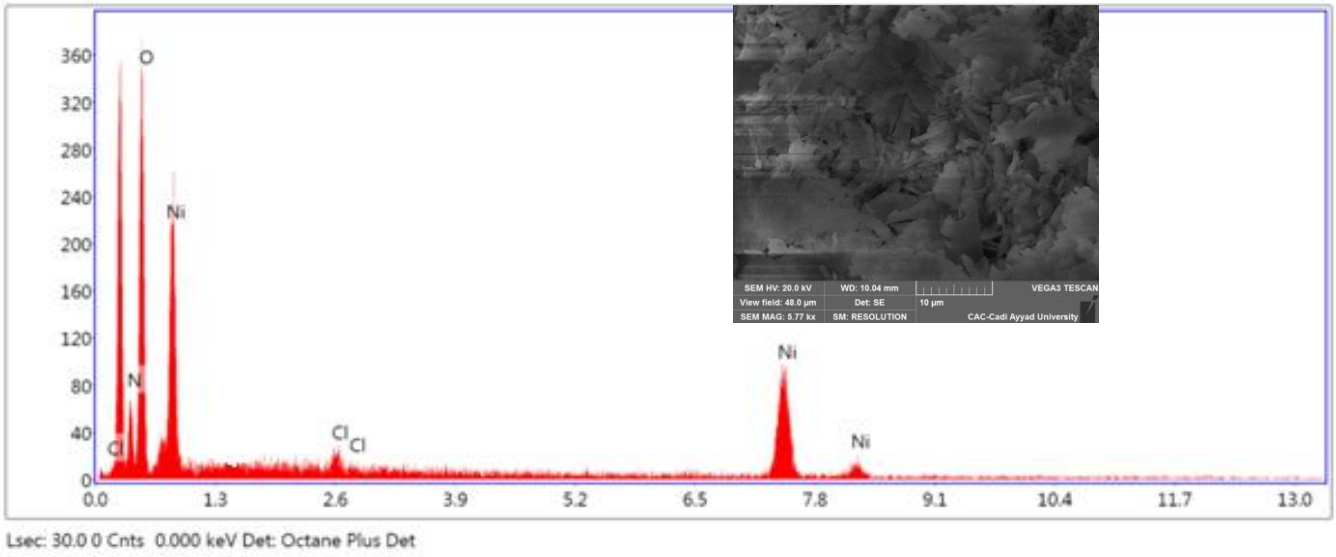

Figure 6: Scanning electron microscopy analysis of the compound $Ni(ala)_2Cl_2$.

Table 4 : Chemical composition of the $Ni(ala)_2Cl_2$complex.

Element	Weight %
N	16.1
O	48.1
Cl	1.0
Ni	34.9

3.6. Electrochemical study

3.6.1. Polarization curves

Figure 7 represents the cathodic and anodic polarization curves of ordinary steel, in 1M HCl, with and without inhibitor at different concentrations, the electrochemical parameters: cathodic Tafel constancy (βc), corrosion potential (Ecorr) and the corrosion current density (Icorr) and inhibition efficiency (IE%°) are given in Table 5.

The inhibitory efficiency IE% of the test compound is defined by the following reaction:

$$IE\% = \frac{I_{corr} - I_{corr/inh}}{I_{corr}} \times 100 \qquad \textbf{(1)}$$

Where I_{corr} and $I_{corr/inh}$ are the corrosion current densities in absence and presence of the inhibitor, respectively

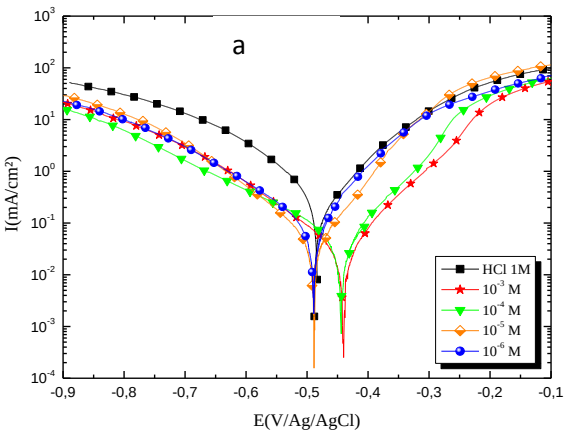

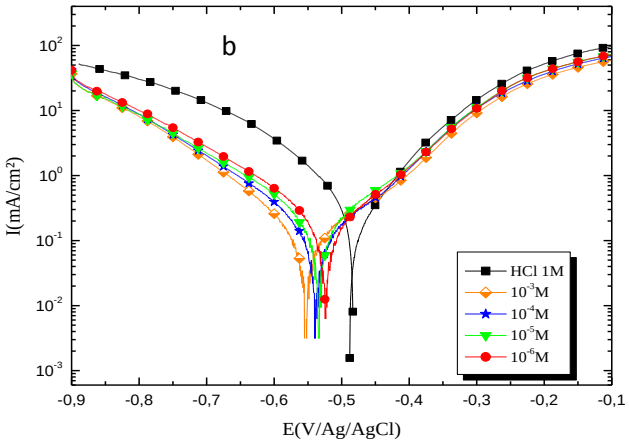

Figure 7: Cathodic and anodic curves of ordinary steel in 1M HCl with and without different concentrations of complex (a) and ligand (b) at 298 K.

Table 5: Electrochemical parameters of ordinary steel at various concentrations of complex in 1.0 M HCl at 298 K

inhibitor	Concentration (M)	E_{corr} (mV/Ag/AgCl)	I_{corr} (µA/cm²)	βc (mV dec^{-1})	IE%
HCl	1.0M	-498	467	-220	-
complex	10^{-3}	-438.9	23	-98.2	95
	10^{-4}	-442.8	30	-92.6	93
	10^{-5}	-487.3	41	-93.5	91
	10^{-6}	-488.0	65	-99.7	86
ligand	10^{-3}	-554.5	92	-104.2	80
	10^{-4}	-539.8	118	-118.4	75
	10^{-5}	-535.3	129	-109.3	72
	10^{-6}	-525.5	149	-118.5	68

- **Case of the complex $Ni(ala)_2Cl_2$**

The polarization curves of ordinary steel in 1M HCl without and with the addition of the complex at different concentrations (Fig.7.a) allow us to observe that the addition of the test compound causes a slight displacement of the corrosion potential towards the cathodic values. This displacement is accompanied by a clear decrease in cathodic and anodic current densities. This result highlights the mixed nature of the used inhibitor.
The electrochemical parameters of the steel in 1M HCl without and with addition of this inhibitor and the values of the inhibitory efficiency are given in Table 5. In the light of the results presented in this table, we note that the inhibitory efficacy increases with the increase of the concentration of the complex and reaches a maximum value of 95% for a concentration equal to 10^{-3} M. This can be explained by the inhibitor molecules adsorption on the metallic surface.

- **Case of the ligand alanine**

The polarization curves of ordinary steel in 1M HCl without and with the addition of the ligand at different concentrations (Fig.7.b) show that the addition of this inhibitor causes a small displacement of the corrosion potential towards more cathodic values. This displacement is accompanied by a decrease in cathodic current. Otherwise, we observe that the Anodic polarization curves are not so much affected by the presence of the ligand, which highlights the cathodic character of the latter.

The electrochemical parameters as well as inhibitory efficiency from the polarization curves are given in Table 5. We see that the inhibitory power of the tested compound increases with its concentration to reach a maximum value of 80 to 10^{-3} M.

3.6.2. Study by the electrochemical impedance spectroscopy (EIS)

The Nyquist diagrams of the ordinary steel immersed in the acid solution without and with addition of different concentrations of two inhibitors are shown in the Figure 8.a.b.
The inhibition efficiency of corrosion of ordinary steel is calculated by charge transfer resistance as follows:

$$IE(\%) = \frac{R_{ct/inh} - R_{ct}}{R_{ct/inh}} * 100 \qquad (2)$$

Where R_{ct} and Rct/inh are the charge transfer resistance in absence and presence of the inhibitor, respectively,

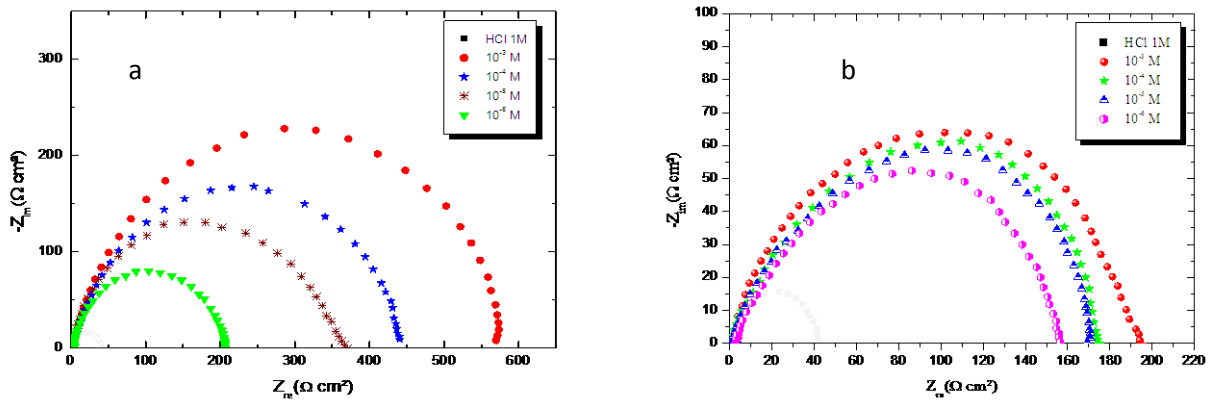

Figure 8: Diagrams of electrochemical impedance of ordinary steel in 1M HCl in the absence and the presence of the complex (a) and ligand (b) at different concentrations and at 298 K.

The values of the electrochemical parameters and the inhibitory efficiency for different concentrations of ligand and complex for the corrosion of ordinary steel in 1M HCl obtained by electrochemical impedance spectroscopy (EIS) are given in the Table 6.

Table 6: Electrochemical impedance parameters of ordinary steel in 1*M* HCl medium in the absence and the presence of the inhibitors at different concentrations at 298 K.

inhibitors	Concentration (M)	Cdl (µF/cm²)	Rct (ohm.cm²)	E%
	HCl 1.0 M	440	40	-
ligand	10^{-3}	53.0	197.0	80
	10^{-4}	58.5	178.4	77
	10^{-5}	59.8	169.3	76
	10^{-6}	103.7	156.4	74
complex	10^{-3}	55.01	578.5	93
	10^{-4}	56.95	441.5	91
	10^{-5}	87.96	361.8	89
	10^{-6}	91.18	204.5	80

From this table, we can make the following observations:

- The values of the transfer resistance (Rt) become greater with the increase of the concentration of the ligand and the complex. The inhibitory efficacy of two inhibitors, calculated from these parameters, evolves in the same way as the charge transfer resistance (Rt) and reaches a maximum value of 80% for the ligand and 93% for the complex at 10^{-3} M.
- With the addition of two inhibitors, the capacity of the double layer (Cdl) decreases from 440 µF.cm^{-2}, for the swing, to 58.5 µF.cm^{-2} for the ligand and 56.95 µF.cm^{-2} for the complex at 10^{-3}M. This decrease is associated with the adsorption of organic molecules on the surface of the steel [37,38,39]. In effect, the more the inhibitor adsorbe, the more the thickness of organic store augments and more the capacity of the double coat diminishes according to the expression of the capacity of the double coat introduced in the model of Helmotz:

$$C_{dl} = \frac{\varepsilon \times \varepsilon_0}{e} \times S \qquad (3)$$

Where e is the thickness of the deposit, S is the surface of the electrode; ε_0 is the permittivity of the medium and ε is the dielectric constant

The results obtained show that the inhibiting action of complex is more efficacy than that of ligand. IE (%) of complex attains a value of 93% at 10^{-3}M for inhibitor in 1M HCl.

3.6.3. Adsorption isotherm and thermodynamic parameters

The rate of recovery θ , is determined by the report (IE%/100) (Table 5). Here, IE% is evaluated from the electrochemical method of polarization curves.

Curves introducing C_{inh}/θ according to C_{inh} are of right (Fig 9) pointing out that the adsorption of these inhibitors makes according to method of isotherm of Langmuir. The strong correlations (R^2 = 0 ,999 for the compound ligand and R^2 = 1 for complex) confirm the validity of this approach. The values of the thermodynamic parameters were calculated from Langmuir model.

$$\frac{C_{inh}}{\theta} = \frac{1}{K_{ads}} + C_{inh} \qquad (4)$$

Where K_{ads} is the adsorption equilibrium constant connected to the free adsorption enthalpy ΔG_{ads} by the relation:

$$K_{ads} = \frac{1}{55,5} \exp\left(-\frac{\Delta G_{ads}}{RT}\right) \qquad (5)$$

Where R is the universal gas constant, T the thermodynamic temperature and the value of 55.5 is the concentration of water in the solution [40].

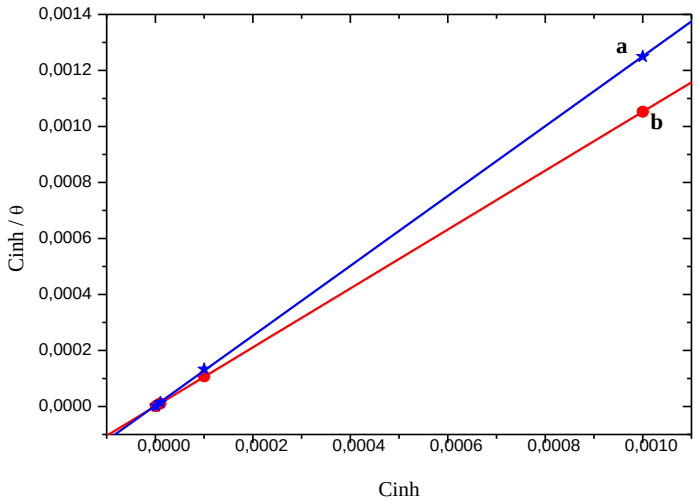

Figure 9: Langmuir adsorption plots for ordinary steel in 1M HCl containing different concentrations of (a) ligand and (b) complex.

The value K_{ads} calculated from the reciprocal of intercept of isotherm line is indicating in the Table 7. The high value of the adsorption equilibrium constant reflects the high adsorption ability of this inhibitor on ordinary steel surface.

Table 7: Thermodynamic parameters for the adsorption of ligand and complex in 1M HCl on the ordinary steel at 298K.

inhibitors	**K_{ads} (L mol^{-1})**	**R^2**	**ΔG_{ads}(KJ.mol^{-1})**
ligand	308641	0 ,999	-41,25
complex	1076426	1	-44,34

The values of ΔG_{ads} are negatives the stability of the adsorbed layer on the steel surface. Generally speaking, the adsorption type is regarded as physisorption if the absolute value of ΔG_{ads} was of the order of 20 kJ mol^{-1} or lower. The inhibition behavior is attributed to the electrostatic interaction between the organic molecules and iron atom. When the absolute value of ΔG_{ads} is of the order of 40 kJ mol^{-1} or higher, the adsorption could be seen as chemisorption. In this process, the covalent bond is formed by the charge sharing or transferring from the inhibitor molecules to the metal surface [41, 42]. Based on the literature [43], the calculated ΔG_{ads} values in this work (Table 7) indicate that the adsorption mechanism of these compounds on ordinary steel in 1M HCl solution is typical of chemisorption. The same conclusion was given by Wang et al [44].

3.6.4. Effet of temperature

Temperature can modify the interaction between the steel electrode and the acidic media without and with inhibitors. Polarization curves for ordinary steel in 1M HCl in the absence and presence of 10^{-3} M of inhibitors in the temperature range 298 K to 328 K are shown in figure 10,11.a.b presented the obtained potentiodynamic polarization curves and their corresponding data are presented in Table 8.

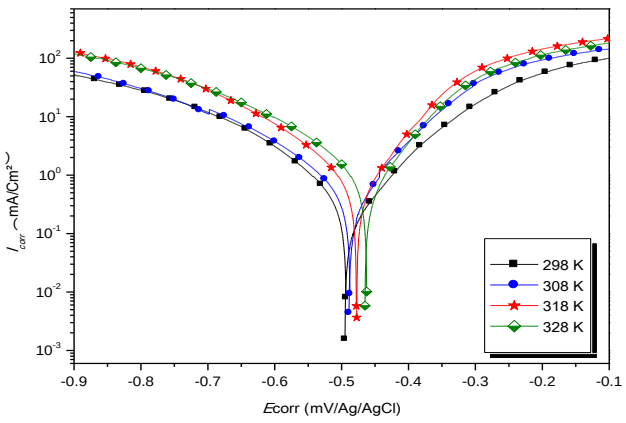

Figure 10: Potentiodynamic polarization curves for ordinary steel in 1M HCl in the absence of inhibitors at different temperatures between 298K and 328K.

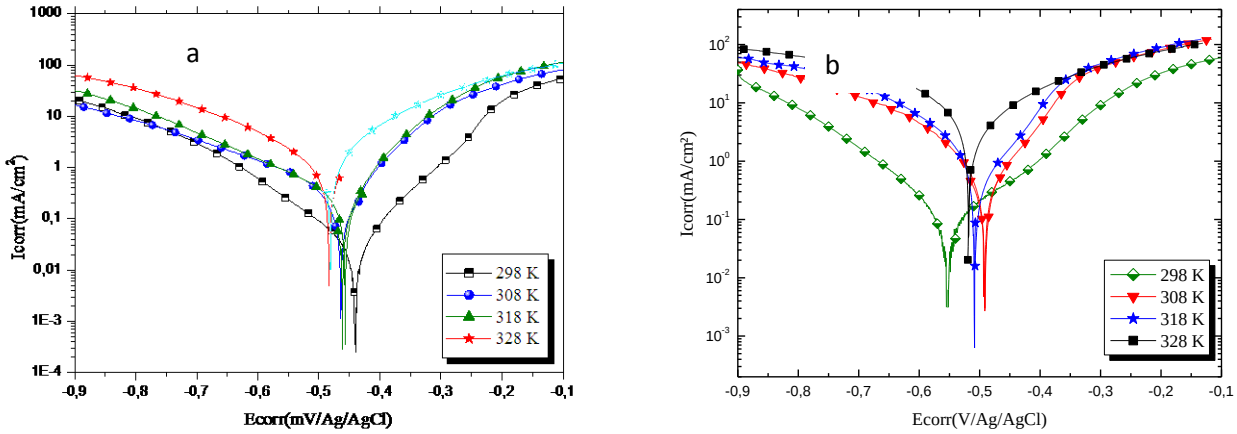

Figure 11.a.b: Potentiodynamic polarization curves for ordinary steel in 1M HCl in the presence of 10^{-3}M of complex (a) and ligand (b) at different temperatures between 298 K and 328 K.

The electrochemical values as well as that of the inhibitory efficiency associated with these measurements are assembled in Table 9.

Table 9: The influence of temperature on the electrochemical parameters for ordinary steel in 1M HCl with 10^{-3} M of ligand and complex.

inhibitors	**T (K)**	**E_{corr} (mV/Ag/AgCl)**		**I_{corr} (µA/cm²)**		**IE (%)**
		blank	10^{-3}M	blank	10^{-3}M	-
ligand	298	-498	-554.5	467	92	80
	308	-491	-490.1	800	421	47
	318	-475	-507.5	1600	894	44
	328	-465	-490.3	2000	1866	7
complex	298	-498	-438.9	467	23	95
	308	-491	-462.6	800	173	78
	318	-475	-455.5	1600	190	88
	328	-465	-481.9	2000	577	71

Results obtained, we can make the following remarks:

- The current densities increase with the increase in the temperature of 298 to 328K, the curves in the cathodic part are parallel, indicating that the reduction of H to the surface of the steel is according to the same pure activation mechanism throughout the temperature range.
- The potential of corrosion of steel (Ecorr) is little changed by the increase in the temperature 298 to 328K in HCl 1 M without and with inhibitors.
- In General, the increase in temperature causes Icorr values increased in the whole field of temperature studied. The evolution of corrosion currents in the corrosive solution (1M HCl) shows a steady and rapid growth, confirming an increasing metallic dissolution with increasing temperature. The increase of the current of corrosion with the temperature in the presence of inhibitors is broadly weaker than in the blank.

3.6.5. Kinetic parameters of activation corrosion process

The activation thermodynamic parameters of the corrosion process can be determined using Arrhenius Eq. (5) [45,46,47,48] and Eq.(6) [49] transition state:

$$I_{corr} = A\exp\left(\frac{-Ea}{RT}\right) \quad (5)$$

Where Icorr is corrosion current, A is the constant, Ea is the activation energy of the metal dissolution reaction, R is the gas constant and T is the temperature.

$$I_{corr} = \frac{RT}{Nh}\exp\left(\frac{\Delta S^{\circ}_{abs}}{R}\right)\exp\left(\frac{-\Delta H^{\circ}_{abs}}{RT}\right) \quad (6)$$

Where N is Avogadro's constant, h is the Plank's constant, $\Delta S^{\circ}_{abs}$is the entropy of activation and ΔH°_{abs} is the enthalpy of activation.

A plot of ln (icorr) vs 1000/T obtained gave a straight line with regression coefficient close to unity, as shown in Figure 12. The Arrhenius plot of $Ln(\frac{I_{corr}}{T})$ vs 1000/T (Figure 12) which gave straight lines with slope ΔH°abs/R and

intercept$\left(\mathrm{Ln}\left(\frac{R}{Nh}\right)+\left(\frac{\Delta S^{\circ}_{abs}}{R}\right)\right)$ from which ΔHa and ΔS°_{abs} values were calculated. The values of Ea, ΔH°_{abs} and ΔS°_{abs} were calculated and tabulated in Table 10.

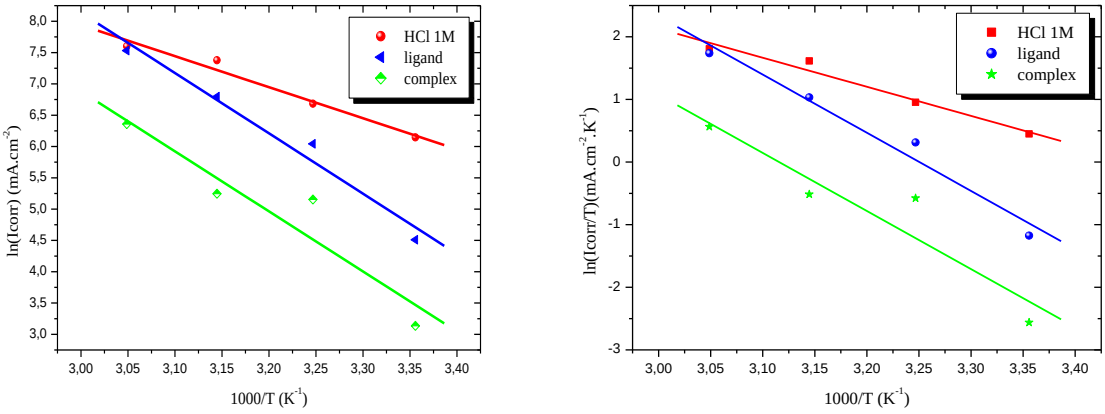

Figure12: Arrhenius plots for ordinary steel in 1M HCl in the absence and presence of 10^{-3} M concentration of ligand and complex.

Table 10: Activation parameters, Ea, ΔH°_{abs} and ΔS°_{abs}, of the dissolution of ordinary steel in 1M HCl in the absence and the presence of 10^{-3} M of ligand and complex.

Inhibitors	**Ea (KJ.mol^{-1})**	ΔH°_{abs} **(KJ. mol^{-1})**	ΔS°_{ads} **(J.mol^{-1}.K^{-1})**
blank	41,1	38,5	-64,4
10^{-3} of ligand	80,1	77,5	54,4
10^{-3}M of complex	79,7	77,1	42,8

From the results in Table 10, we notice that:

The studied inhibitors are adsorbed on the surface by electrostatic bonds (physisorbed on the surface of the electrode). Indeed, the Ea value for ligand and complex is greater than the Ea value which is obtained for the solution without inhibitors.

The positive signs of enthalpies ΔH°_{abs} reflect the endothermic nature of the steel dissolution process. Indeed, the increase in the enthalpy of activation $\Delta H^{\circ}_{abs}$with the concentration corresponds to a decrease in the dissolution of the metal [50].

The values of ΔS°_{ads} in the presence of ligand and complex (Table 9) are broad and positive explained by an increase in disorder taking place by reagents in the reaction complex of the adsorbed species of metal [51,52,53].

3.7. Scanning electron microscopy (SEM) energy dispersive X-ray (EDX) analysis

In order to confirm the obtained results with electrochemical measurements. Qualitative microscopic analyses of MEB coupled with quantitative analyses EDX have been done. Figure 19 shows MEB micrographs of the steel surface, before and after exposed in 1M HCl medium during 6 hours at T=298K, in absence and presence of both inhibitors. The characteristics of the parallel treatment on the polished surface of ordinary steel before to immersed in the corrosive solution are clearly visible in the image of ordinary steel only, which is associated with scratch friction.

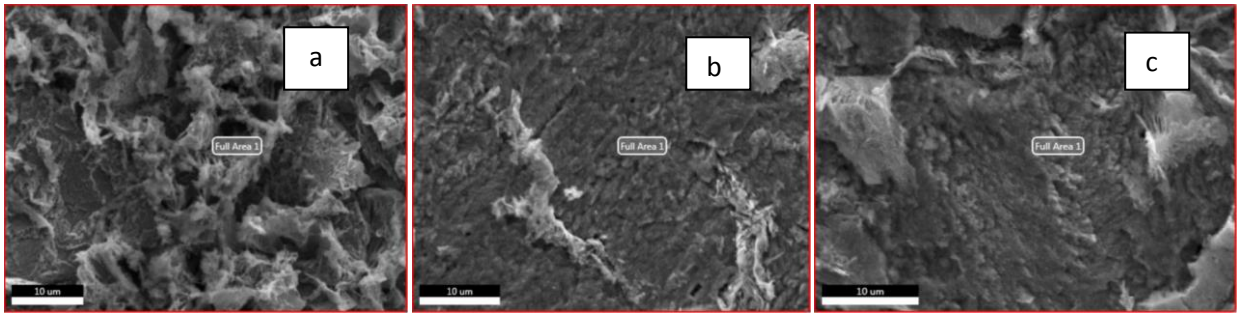

Figure 13: Micrograph (SEM) of the surface of ordinary steel (a) after 6 h immersion in 1M HCl in the absence and in the presence of inhibitors alanine (b) and $Ni(ala)_2Cl_2$ (c) 10^{-3}M at 25 °C.

The morphology of the exposed surface to 1M HCl solution without inhibitor (Fig 13) exhibits a heterogeneous layer of corrosion products. In fact, the MEB micrographs in presence of inhibitors alanine and $Ni(ala)_2Cl_2$ shows that the

surface is covred by the corrosion products and reveal the formation of a protective layer of these compounds adsorbed on the surface the ordinary steel [54].

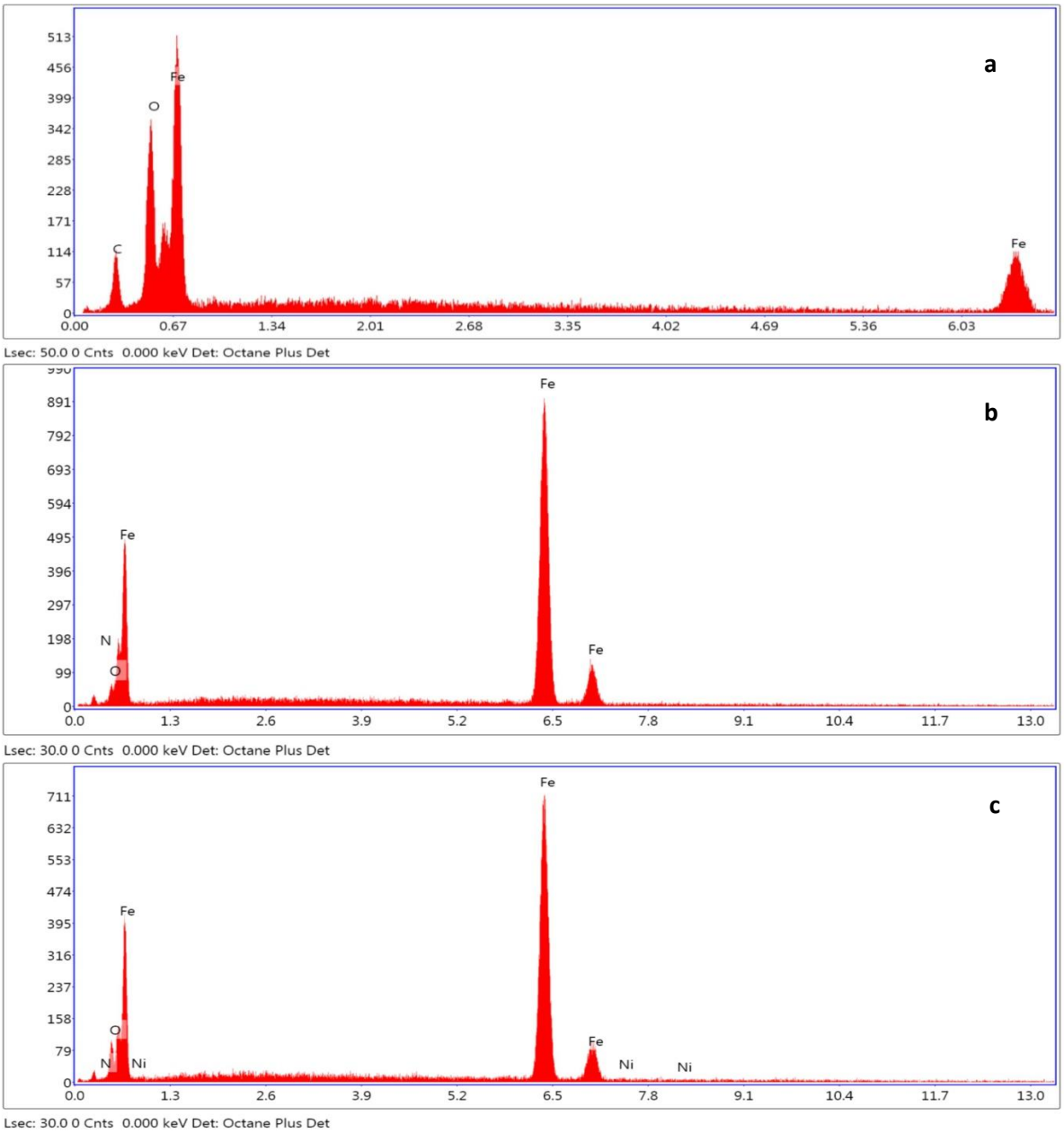

Figure 13: Spectra EDX of the surface of ordinary steel after immersion in 1M HCl (a) in the presence of ligand (b) and complex (c) 10^{-3} M at 25 ° C.

Table 10: Percentage mass different existent elements of the analysis EDX of the surface of ordinary steel in HCl 1M in absence and in the presence of inhibitors alanine and $Ni(ala)_2Cl_2$ 10^{-3}M à 25 °C.

Element	Weight %		
	ordinary steel	alanine	$Ni(ala)_2Cl_2$
C	11.5	0	0
O	19.3	2.4	4.5
Fe	69.2	96.4	93.0
N	0	1.2	0.9
Ni	0	0	1.7

EDX analyses (Fig.13) shows a decrease in the peaks of O atoms and apparition of peaks of Nitrogen N, indicating that the molecules of the products alanine and $Ni(ala)_2Cl_2$ are strongly adsorbed on the metal surface and justify the inhibitory role of this product (Table 10) [55]. As a consequence, these results confirm those obtained with electrochemical measurements.

4. CONCLUSION

In this work, the complexation of alanine with anhydrous nickel chloride was studied. The isolated complex $Ni(ala)_2Cl_2$ with a yield equal to 82% was characterized by the UV-visible spectroscopy , the infrared spectroscopy and the scanning electron microscopy (SEM) energy dispersive X-ray (EDX) analysis.

Also the corrosion inhibition efficiency of complex and ligand on ordinary steel in 1M HCl was investigated by electrochemical measurements. It is found that the complex and ligand show a good inhibition performance for ordinary steel in 1M HCl solution and its inhibition efficiency increase with concentrations and decrease with temperature. It is found that the complex acts as a mixed-typed inhibitor while the ligand acts as a cathodic inhibitor. And its adsorption on the ordinary steel surface obeys Langmuir adsorption isotherm.

The study of morphology of the surface steel by MEB coupled with the EDX shows the existence of a stable and insoluble adherent deposit which limits the access of the electrolyte to the surface of the metal.

5. REFERENCES

1. Asemave K, Yiase SG, Adejo SO. Kinetics and Mechanism of Substitution Reaction of Trans-Dichloro-bis-(Ethylenediammine) Cobalt (III) Chloride with Cysteine, Aspartic acid and Phenylalanine. *International Journal of Science and Technology*. 2012; (**2):** 2224.
2. Tripathi IP, Aarti K. Synthesis, Characterization of Some Complexes of Copper (II) with L-Asparginine, L-Histidine, L-Lysine. *American Journal of Advanced Drug Delivery*.2015; **(3)**: 103.
3. Rayan AM, Ahmed MM, Barakat MH, Abdelkarim AT, El-Sherif AA. Complex formation of cetirizine drug with bivalent transition metal (II) ions in the presence of alanine: synthesis, characterization, equilibrium studies, and biological activity studies. *Journal of Coordination Chemistry***.** 2015; **(2):** 26.
4. Naglah AM, Al-Wasidi AS, Al-Jafshar NM, Al-Otifi JS, Refat MS, Hassan RF, Hozzein WN. Synthesis, characterization and antioxidant measurements of selenium (IV) complexes with some amino acids-binuclear complexes. *Bulgarian Chemical Communications*. 2018; (**50):** 351.
5. Leung CH, Lin S, Zhong HJ, Ma DL. Metal complexes as potential modulators of inflammatory and autoimmune responses. *Chem Sci.* 2015 ; **(2)**: 884.
6. Marcu A, Stanilaa A, Cozar O, David L. Structural investigations of some metallic complexes with threonine as ligand. Journal of Optoelectronics and Advanced Materials. 2008; (**10):** 833.
7. Hadjer F, Tahar B, Djallal. Eddine A, Sofiane D. Antioxidant and Antimicrobial Activity of Some Transition Metal Complexes with Non-natural Amino Acids Used As Ligand. *J. Mater. Environ. Sci*., 2018 ; **(9)** :2157
8. Bastug A.S, Goz SE, Talman Y, Gokturk S, Asil E, Caliskan E . Formation constants and coordination thermodynamics for binary complexes of Cu(II) and some α-amino acids in aqueous solution. Journal of Coordination Chemistry, 2011; (**64)** : 292
9. Dinelli LR, Bezerra M, Sene JJ. A Kinetic Study of the Reaction between trans- [CoCl2(en)2]Cl and the Amino-acids Alanine and Valine. *Curr. Res. Chem.* 2010; (**2):** 23.
10. Asemave K, Yiase SG, Adejo SO. Kinetics and Mechanism of Substitution Reaction of Trans-Dichlorobis (Ethylenediammine) Cobalt (III) Chloride with Cysteine. *J. Modern Org. Chem*. 2012; (**1):** 9.
11. Dara SS. A textbook of Environmental Chemistry and Pollution Control, S. Chand and Company. *J. Ltd, India*. 2005; (**67):** 69.
12. Gharda N, Galai M, Saqalli L, Ouakki M, Habbadi N, Ghailane R, Souizi A, EbnTouhami M, Peres-lucchese Y. *oriental journal of chemistry*. 2017; **(4)**: 1676
13. Khaled KF, Babic-Samardzija K, Hackerman N. Cobalt (III) complexes of macrocyclic-bidentate type as a new group of corrosion inhibitors for iron in perchloric acid. *J. Corros. Sci*. 2006; (**48):** 3014.
14. Singh VP, Singh P, Singh AK. Synthesis, structural and corrosion inhibition studies on cobalt (II), nickel (II), copper (II) and zinc (II) complexes with 2-acetylthiophene benzoylhydrazone. *Inorg. Chim. Acta***.** 2011; **(56):** 379
15. Kiruthikajothi K, Chandramohan G, Jayabharathi G. Studies on Inhibition of Mild Steel Corrosion by Copper (II) Complexes with some Amino Acids. *Chem Sci Rev Lett*. 2014; (**3):** 607.
16. Ropital F. Current and future corrosion challenges for a reliable and sustainable development of the chemical, refinery, and petrochemical industries mater. *Corros*. 2009; (**60):** 500.
17. Finšgar M, Jackson J. Application of corrosion inhibitors for steels in acidic media for the oil and gas industry: A review. *Corros. Sci*. 2014; (**86):** 41.
18. Saqalli L, Galai M, Benhiba F, Gharda N, Habbadi N,Ghailane R, Ebn Touhami M, Peres-lucchese Y, Souizi A,Touir R. Experimental and theoretical studies of Alizarin as corrosion inhibitor for mild steel in 1.0 M HCl solution. *Journal of Materials and Environmental Sciences*. 2017; (**8):** 2467.
19. Shaban SM, Saied A, Tawfik SM, Abd-Elaal A, Aiad I. Corrosion inhibition and biocidal effect of some cationic surfactants based on Schiff base. *J. Ind. Eng. Chem*. 2013; (**19):** 2009.
20. Medhat I, Abdallah N, Diaa Eldin K. Density functional theory and FTIR spectroscopic study of carboxyl group. *India Journal of pure and Applied Physics*. 2005; (**43):** 917.
21. Wang G, Ma S, Wang J, Miao F. Novel Complexes of Copper(II), Zinc(II), Nickel(II) and Cobalt(II) with the Schiff Base Derived from 2,4-Dihydroxybenzaldehyde and Glycyl-DL-Alanine. synth. react. inorg. met.-org. chem, 1999; **29:** 1031
22. Totta X, Papadopoulou AA, Hatzidimitriou AG, Papadopoulos A, Psomas G. Synthesis, structure and biological activity of nickel(II) complexes with mefenamato and nitrogen-donor ligands. *J Inorg Biochem.* 2015; **(145)**: 93.
23. Sharma RP, Saini A, Singh S, Venugoplalan P, Ferretti V. Two new second sphere coordination complexes of copper(II): Syntheses, characterization, single crystal structure and packing analyses of $[trans\text{-}Cu(en)_2(H_2O)_2](L_1/L_2)_2$ where L_1 = 3-methoxybenzoate, L_2 = 3,4,5-trimethoxybenzoate. *Journal of Molecular Structure*. 2010; (**979):** 135.
24. Mrozek R, Rzaczynska Z, Sikorska-Iwan M, Jaroniec M, Iowiak TG. synthesis and crystal structure of [bis (dl-alaninato) diaqua] nickel (ii) dihydrate. *Polyhedron*. 1999; (**18):** 2321.
25. Brisdon A. Kazuo Nakamoto Infrared and Raman Spectra of Inorganic and Coordination Compounds, Part B, Applications in Coordination, Organometallic, and Bioinorganic Chemistry, 6th edn Wiley. *Appl. Organometal. Chem.* 2010; **(24)** : 489
26. Masoud MS, Amira MF, Ramadan AM, El-Ashry GM. Synthesis and characterization of some pyrimidine, purine, amino acid and mixed ligand complexes. *Spectrochimica Acta Part A*. 2008; (**69):** 238.
27. Alaghaz AMA, Bayoumi HA. Synthesis, Spectral Properties and Potentiometric Studies on Some Metal Schiff Base Complexes Derived from 4–chlorophenyl–2–aminothiazole. *Int. J. Electrochem. Sci*.,2013 ; **(8)** :11876
28. Dilip CS, Thangaraj V, Raj AP. Synthesis, spectroscopic characterisation, biological and DNA cleavage properties of complexes of nicotinamide. *Arabian Journal of Chemistry*. 2016; (**9):** 742.
29. Rafat F, Siddiqi MY, Siddiqi KS. Synthesis and characterization of Ni(II), Cu(II) and Co(III) complexes with polyamine-containing macrocycles bearing an aminoethyl pendant arm. *J. Serb. Chem. Soc.* 2004 ; **(69)** : 641
30. Sacconi L. Tetrahedral complexes of nickel (II) and copper (II) with Schiff bases. *Coord. Chem. Revs*. 1966 ; (**1):** 192.
31. Al-Qudsi ZN, Abood HMA. The Electronic Transition Behavior Cr (III), Fe (III), Fe (II) and Ni (II), Transition Metal Cations In Ammonium Alum-Urea Room Temperature Ionic Liquid. *Journal of Al-Nahrain University*. 2013; (**16):** 55.
32. Mohamed GG, Abd El-Wahab ZH. Salicylidene-2- Aminobenzimidazole Schiff Base Complexes of Fe(III), Co(II), Ni(II), Cu(II), Zn(II) AND Cd(II). Journal of Thermal Analysis and Calorimetry. 2003; **(73)**: 359

33. *SHAKER SA. Preparation and Study of Some Mn(II), Co(II), Ni(II), Cu(II), Cd(II) and Pb(II) Complexes Containing Heterocyclic Nitrogen Donor Ligands. E-Journal of Chemistry.* 2010 ; **(4)** : 1598.
34. Sawant V, Gotpagar S, Yamamgar B, Sawant S, Kankariya R, Chavan S. Characterization and electrochemical studies of Mn (II), Co (II), Ni (II) and Cu (II) complexes with 2-mercapto-3-substituted-quinazolin-4-one and 1, 10-phenanthroline or ethylenediamine as ligands. *Spectrochimica Acta Part A.* 2009; **(72):** 669.
35. Rondi A, Rodriguez Y, Feurer T, Cannizzo A. Solvation-Driven Charge Transfer and Localization in Metal Complexes. *Acc. Chem. Res*. 2015; **(48):** 1440.
36. Musa TM, Al-jibouri MNA, Abbas BF. Synthesis, Characterization and Thermal Study of Some Transition Metal Complexes Derived from Quinoxaline-2,3-Dione. Ibn Al-Haitham Journal for Pure and Applied science. 2017 ; **(10)** :526
37. Khan MM. Ru(III), Pd(II), Pt(III), and Pt(IV) Complexes of a Novel 32-Membered Unsymmetrical Dinucleating Macrocyclic Ligand. *Synthesis and Reactivity in Inorganic, Metal-Organic, and Nano-Metal Chemistry*, 2010; **(40)**: 152
38. Benali O, Benmehdi H, Hasnaoui O, Selles C, Salghi R. Green corrosion inhibitor: inhibitive action of tannin extract of Chamaerops humilis plant for the corrosion of mild steel in 0.5 M H2SO4. *J. Mater. Environ. Sci*. 2013; **(4):** 138
39. Ben Hmamou D, Salghi R, Zarrouk A, Benali O, Fadel F, Zarrok H, Hammouti B. Carob seed oil: an efficient inhibitor of C38 steelcorrosion in hydrochloric acid. International Journal of Industrial Chemistry, 2012; **(3):** 25.
40. Machnikova E, Whitmire KH, Hackerman N. Corrosion inhibition of carbon steel in hydrochloric acid by furan derivatives. *Electrochim. Acta*. 2008; **(53):** 6032.
41. Szklarska-Smialowska Z, Mankowski J. Crevice corrosion of stainless steels in sodium chloride solution. *Corros. Sci.* 1978; **(18):** 960
42. Yurt A, Ulutas S, Dal H. Electrochemical and theoretical investigation on the corrosion of aluminium in acidic solution containing some Schiff bases. *Appl. Surf. Sci*. 2006; **(253):** 925
43. Hongbo F. Synthesis and Application of New Type Inhibitors, Chemical Industry Press, Beijing, 2002; 166.
44. Wang HL, Fan HB, Zheng JS. Corrosion inhibition of mild steel in hydrochloric acid solution by a mercapto-triazole compound. *Mater. Chem. Phys.* 2003; **(77):** 661.
45. Messaadia L, ID El mouden O, Anejjar A, Messali M, Salghi R, Benali O, Cherkaoui O, Lallam A. Adsorption and corrosion inhibition of new synthesized Pyridazinium-Based Ionic Liquid on Carbon steel in 0.5 M H2SO4. *J. Mater. Environ. Sci*. 2015; **(6):** 598.
46. Labriti B, Dkhireche N, Touir R, Ebn Touhami M, Sfaira M, El Hallaoui A, Hammouti B, Alami A Synergism in Mild Steel Corrosion and Scale Inhibition by a New Oxazoline in Synthetic Cooling Water. *Arabian Journal for Science and Engineering*. 2012; **(37):** 1303
47. Li X, Deng S, Fu H. Benzyltrimethylammonium iodide as a corrosion inhibitor for steel in phosphoric acid produced by dihydrate wet method process. *J. Corros Sci*. 2011; **(53):** 670.
48. Li X, Deng S, Fu H Allyl thiourea as a corrosion inhibitor for cold rolled steel in H3PO4 solution. *Corros Sci*. 2012; **(55)**: 288.
49. Musa A, Mohamad AB, Kadhum AAH, Takriff MS, Tien LT. Synergistic effect of potassium iodide with phthalazone on the corrosion inhibition of mild steel in 1.0M HCl. *J. Corros Sci.* 2011 ; **(53):** 3672.
50. Tazouti A, Galai M, Touir R, Ebn Touhami M, Zarrouk A, Ramli Y, Saraçoğlu M, Kaya S, Kandemirli F, Kaya C. Experimental and theoretical studies for mild steel corrosion inhibition in 1.0 M HCl by three new quinoxalinone derivatives. *Journal of Molecular Liquids*. 2016; **(221):** 832.
51. Alaoui K, El Kacimi Y, Galai M, Dahmani K, Touir R, El Harfi A, Ebn Touhami M. Anti-corrosive properties of polyvinyl-alcohol for carbon steel in hydrochloric acid media: electrochemical and thermodynamic investigation. *Anal. Bioanal. Electrochem*. 2016; **(8):** 830
52. Tiskar M, Galai M, Elhadiri H, Ebn Touhami M, Sfaira M, Satrani B, Ghanmi, M, Chaouch A, Touir R. Juniperus Phoenicea essential oil as green corrosion inhibitor for mild steel in molar hydrochloric acid. *Matériaux & Techniques.* 2016 ; **(104):** 609.
53. Ismaily Alaoui K, Ouazzani F, kandrirodi Y, Azaroual AM, Rais Z, Filali Baba M, Taleb M, Chetouani A, Aouniti A, Hammouti B Effect of some Benzimidazolone compounds on C38 steel corrosion in hydrochloric acid solution. *J. Mater. Environ. Sci*, 2016; **(7):** 258.
54. Ouakki M, Rbaa M, Galai M, Lakhrissi B, Rifi EH, Cherkaoui M. Experimental and Quantum Chemical Investigation of Imidazole Derivatives as Corrosion Inhibitors on Mild Steel in 1.0 M Hydrochloric Acid, *Journal of Bio- and Tribo-Corrosion*. 2018 ; **(4)** 35
55. Devi AR, Ramesh S, Periasamy V. corrosion protection of copper using amino acid self-assembled monolayers. Journal of Science. 2015; **(5)** : 598.

Cite this article: Nadia Gharda, Mouhsine Galai, Lamyae Saqalli, Moussa Ouakki, Rachida Ghailane, Mohamed EbnTouhami, Abdelaziz Souizi, and Nouzha Habbadi. COMPARATIVE CORROSION INHIBITION STUDY OF ORDINARY STEEL IN 1M HCL DL- A -ALANINE AND BIS Ni(ALA)2CL2 COMPLEX SYNTHESIS. *Am. J. innov. res. appl. sci. 2019; 8(4): 131*-x144.